ENGINEERING RESEARCH JOURNAL (ERJ)
Vol. 51, No. 3 July. 2022, pp.105-119
Journal Homepage: http://erj.bu.edu.eg

# Flexural Behavior of Reinforced Concrete Beams with Geogrid - Experimental Study

**Mona K. N. Ghali [a], Mohamed Said [b], Sherif El-Beshlawy [c], Reham Mahmoud [d *]**

[a]Professor of Reinforced Concrete Structures, Civil Eng. Dep., Shoubra Faculty of Eng/ Benha University, Egypt
[b]Professor of Reinforced Concrete Structures, Civil Eng. Dep., Shoubra Faculty of Eng/ Benha University, Egypt
[c]Lecturer, Construction Engineering Department, The Higher Institute of Eng/ 6th of October City, Egypt)
[d]Construction Engineering Department, The Higher Institute of Eng/ 6th of October City, Egypt)
*Corresponding auher

**Abstract**

Geogrids are categorized as one of the geosynthetics materials that are used for soil stabilization and reinforcing of earth structures such as earth walls and dams. This research investigated the effect of using uniaxial geogrids as additional reinforcement, in addition to, steel fibers in the concrete mix, on the flexural behavior of beams. The experimental research work comprised of testing thirteen simply supported reinforced concrete (R.C) beams which were tested up to failure under four-point loading. The variables of this study are: the volume of steel fibers (0.0, 0.5, 1.0 %), number of geogrid layers (one, two, and three layers), the shape of the geogrid layers, and the longitudinal reinforcement percentage. The mid-span deflection, failure loads, ductility, crack patterns, steel, concrete and Geogrid strains of the beams were reported and compared. The test results concluded that the addition of Geogrid layers as a reinforcing technique proved to be an effective tool to improve the flexural behavior of R.C beams and improve the cracking patterns. The number of geogrid layers used in the beams plays a significant effect in increasing the failure loads and decreasing the deflections of the beams. The addition of steel fibers in R.C beams, in addition to, Geogrid layers increases the cracking loads, failure loads and reduces the deflection of beams at failure loads. Increasing the fiber content from (0.5%) to (1%) had a slight effect on increasing the maximum carrying capacities of the beams. Addition of U-shaped Geogrid layers had a considerable effect on increasing the failure loads rather than the addition of Geogrid layers in the tension zone only.

**Keywords** : Beams, Flexural behavior; Geogrids and Steel fibers.

## 1. Introduction

Geogrids are a geosynthetics material made from polymers like polyester, polypropylene, and polyethylene [1,2].

Geogrids are used as stabilization and strengthening elements of soil and important civil works. Geogrids are now being used as a reinforcement material for pavement networks, and reinforcing parts of asphalt layers in particular.

Geogrids are being explored for their potential as being used as a replacement of rigid pavements because of their significantly greater strength-to-

weight ratio, comparatively low cost, and ease of handling [3]. Three major categories of geogrids are (uniaxial, biaxial, and triaxial) geogrids. The classifications of geogrids are shown in Figure 1. Uniaxial geogrids are used in steep slopes and retaining walls and can mostly be used for grade separation purposes, whereas biaxial and triaxial geogrids are utilized mostly for roadway applications [4].

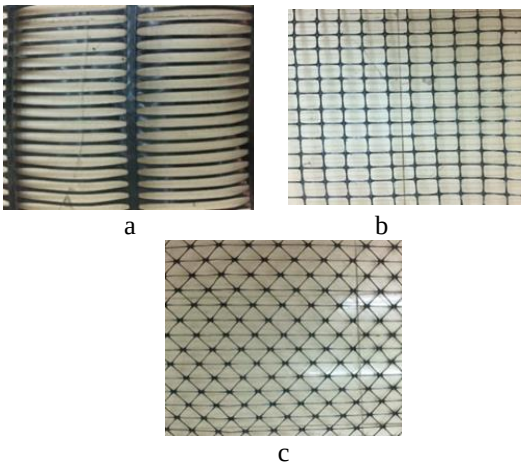

a b c

**Fig.1** The types of geogrids.

Chehab and El-Meski (2014) [4] used different types of geogrids in order to study samples of concrete beams tested under four-point loading. All geogrid reinforced specimens showed a significantly greater deflection at maximum load, showing the behavior of ductile post cracking compared to the load deflection of control specimens. Geogrids makes building easier because they could be installed under any climatic conditions and enable the unsuitable soil to be better prepared for requirements of building [1,5]. The using of geogrid increases the amount of available land by allowing for the construction of steep slopes or walls, allowing a highway to be built on the ground under weak conditions. Finally, geogrids have been used as reinforcements in networks of pavements, especially for material stabilization in unbound surfaces, and element reinforcement in layers of the asphalt [6–11].

Many researches have examined the behavior of strengthened or reinforced concrete elements with FRP like glass and carbon fibers [12–15]. To evaluate the effectiveness of geogrids in preventing cracking, Itani, et al. (2016) [16] used uniaxial geogrid thin concrete overlays. The research results reported that geogrids layers assisted concrete with extra load capacity after cracking and ductility. Geosynthetics have widely been used in geotechnical applications. They are utilized as reinforcement elements to achieve stabilization of soil [17].

Geogrids have been effectively utilized to enhance soft subgrades and provide a construction platform over them [18, 19]. Al-Hedad, et al. (2017) [20] studied beam and slab specimens reinforced with biaxial geogrid layers to evaluate the effect of geogrid usage on the drying shrinkage behavior concrete pavements. The research results concluded that geogrids reduced the drying shrinkage strains by 7 % to 28 % compared to control concrete samples. Chidambaram and Agarwal (2014) [21] studied the behavior of cylindrical specimens under flexural and compressive loading to stabilize concrete samples with geogrids. The results indicated that the use of geogrid layers in concrete specimens showed much improvement in the concrete behavior relative to standard reinforcements.

Kim, et al. (2008) [22] studied the behavior of R.C samples using one and two layers of flexible and rigid biaxial geogrids. The results concluded that the rigid geogrids have better results compared to flexible geogrids. Beebi and Visweswara. [23], Santosh, et al. [24], Shobana and Yalamesh [25], Rakendu and Manoharan [26], and Ghodmare, et al. [27] examined the behavior of reinforced beams with geogrids. The results of these researches were:

- The number of geogrid layers and geogrid strength significantly effects load deflection and flexural strength.
- Compared to beams reinforced without geogrids, geogrid reinforcement enhances ductile behavior, deflection, and flexural strength.
- Uniaxial, biaxial and triaxial geogrids provided post-cracking in beams like steel.
- By using the geogrids in beams, deflection can be decreased.

Ahmed Shaban Abdel-Hay (2019) [28] studied different types of geogrids to strengthen reinforced concrete slabs. It was found that, compared to traditional strengthening techniques, geogrids can be considered as a useful alternative material for strengthening reinforced concrete slabs. The use of geogrids as a reinforcement technique increased the slabs' flexural strength and decreased the deflection at failure load.

In additional of using geogrids and steel fibers for strengthening reinforced concrete beams, there are many materials also used for that purpose such as ferrocement [29].

## 2. Properties of Materials

A detailed description of the materials used in the present research work are here-in presented. The properties of concrete, steel fibers, and geogrids materials are summarized as follows.

### *2.1. Reinforced concrete materials*

The properties of cement, coarse aggregate, sand and steel used in the reinforced concrete beam specimens were tested according to ECCP 203-2020 [30].

**Table 1.** Concrete mix content by weight for one cubic meter of concrete.

| Material | Quantity |
|---|---|
| Cement (Kg/ $m^3$) | 360 |
| Sand (Kg/ $m^3$) | 685 |
| Water (Liter/ $m^3$) | 190 |
| Coarse aggregate (Kg/ $m^3$) | 1120 |
| Admixture (Liter/ $m^3$) | 0.5 |

A total of 39 samples were used for the tested mixture. Three cubes with dimensions 150 x150x150 were used for every sample. The concrete strength was determined by testing the cubes after 28 days. The cube compressive strength of the concrete was 40MPa after 28 days. Deformed high tensile steel bars of 10 and 12 mm diameter with yield strength of 360 MPa and ultimate strength of 520 MPa was used. The modulus of elasticity of reinforcing bars was 2.1x103 MPa.

*2.2. Steel fibers*

Steel fibers are reinforcement materials made of cold drawn wire and then shaped to improve concrete mechanical properties. Corrugated Round Steel Fibers used in the experimental program were manufactured by Nassar group (MF) company and have the following properties. The length of each fiber was 50mm. The diameter was 1mm and the tensile strength was 1100 N/ mm2. Fig. 2 shows the steel fiber details.

*2.3. Geogrids*

Uniaxial geogrids with a tensile strength of 160 [kN/m] was used in this study. Uniaxial geogrids used in the experimental program were manufactured by (Geos) company. Figure 3 shows the uniaxial geogrids used in the experimental work. Uniaxial geogrids are manufactured with a unique extrusion technology using high-quality polymers, high tensile modulus, great interlock capacity and junction strength, and superior long-term design strength and durability. Geogrid properties are shown in Table.2.

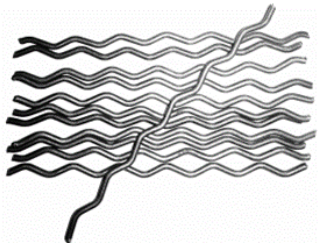

**Fig.2** Steel fibers used in all specimens

**Fig.3** Uniaxial geogrids used in specimens

**Table 2.** physical and Mechanical properties of geogrid

| Component | Description | Unit |
|---|---|---|
| | Uniaxial | |
| Tensile Strength at (2% strain) | 45 | kN/m |
| Tensile Strength at (5% strain) | 90 | kN/m |
| Peak tensile strength | 160 | kN/m |
| Yield point elongation | 13 | % |
| Junction strength | 130 | kN/m |

## 3. Experimental work

The experimental study was examined the flexural behavior of R.C beams reinforced with uniaxial geogrids and steel fibers. Specimens were tested under four-point loads. All specimens were constructed in the R.C. laboratory of the Housing and Building National Research Center. One concrete mix has been used. The specimens were removed and cured by wet canvas for 28 days before testing.

*3.1. Specimen details*

A total of thirteen specimens with and without geogrids and steel fibers were tested. All tested beams were of a constant cross-section of 150×300 mm and total length 2100 mm. Beams were supported with an effective span 1900 mm. The specimens were divided into four groups, in addition to, the control specimens B1 and B2. Group A (B3, B4, and B5) were reinforced with a volume of steel fiber (1%) and uniaxial geogrid layers from one to three layers, respectively.

Group B (B6, B7, and B8) have different longitudinal steel reinforcement than Group A; where specimen B6 was reinforced with a volume of steel fiber (1%) and without geogrid layers. Specimens (B7 and B8) were reinforced with a volume fraction of steel fiber (1%) and uniaxial geogrid layers were used from one to two layers, respectively.

Group C (B9, B10, and B11) were reinforced with a volume of steel fiber (0.5%) and using uniaxial geogrids one to three layers, respectively. Specimens

in Group D (B12 and B13) were reinforced with a volume of steel fiber (1%) and using uniaxial geogrid layers one and two layers (U shaped) having a leg of 200mm extending on each side.

The strain of the lower longitudinal bars and geogrid layers were measured using an electrical-resistance strain gauge 10 mm in length attached at mid-span. An automatic data-logger system connected to a computer was used to monitor deflection, loading, and strains in the reinforcement.

All specimens were reinforced with two steel bars of 10 mm diameter as longitudinal bottom reinforcement, two steel bars of 10 mm diameter as top reinforcement, and 8 mm diameter stirrups at 100 mm center to center spacing as reinforcement for shear; except Group B which were reinforced with three steel bars of 12 mm diameter as longitudinal bottom reinforcement and two steel bars of 10 mm diameter as top reinforcement. The specimens were reinforced with uniaxial geogrids at its bottom. The spacing between geogrid layers is 8 mm. The volume of steel fiber in the concrete mix was 0.5% and 1%. Figure 4 and Table 3 illustrate the details of the tested specimens.

**Table 3.** Test specimens' classification

| Group | Specimen | No of layer (geogrid) | Fiber content Vf (%) | Bottom RFT | Top RFT | Stirrups |
|---|---|---|---|---|---|---|
| **Control** | B1 | ---- | 0% | 2 ø 10 | 2 ø 10 | 10 ø 8 |
| **Control** | B2 | | 1% | 2 ø 10 | 2 ø 10 | 10 ø 8 |
| **A** | B3 | 1 | 1% | 2 ø 10 | 2 ø 10 | 10 ø 8 |
| | B4 | 2 | 1% | 2 ø 10 | 2 ø 10 | 10 ø 8 |
| | B5 | 3 | 1% | 2 ø 10 | 2 ø 10 | 10 ø 8 |
| **B** | B6 | ---- | 1% | 3 ø 12 | 2 ø 10 | 10 ø 8 |
| | B7 | 1 | 1% | 3 ø 12 | 2 ø 10 | 10 ø 8 |
| | B8 | 2 | 1% | 3 ø 12 | 2 ø 10 | 10 ø 8 |
| **C** | B9 | 1 | 0.5% | 2 ø 10 | 2 ø 10 | 10 ø 8 |
| | B10 | 2 | 0.5% | 2 ø 10 | 2 ø 10 | 10 ø 8 |
| | B11 | 3 | 0.5% | 2 ø 10 | 2 ø 10 | 10 ø 8 |
| **D** | B12 | 1 (U shape) | 1% | 2 ø 10 | 2 ø 10 | 10 ø 8 |
| | B13 | 2 (U shape) | 1% | 2 ø 10 | 2 ø 10 | 10 ø 8 |

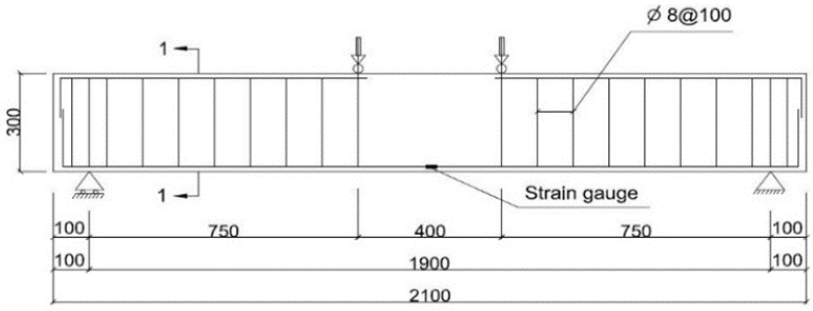


Longitudinal Section For TheTested Beams

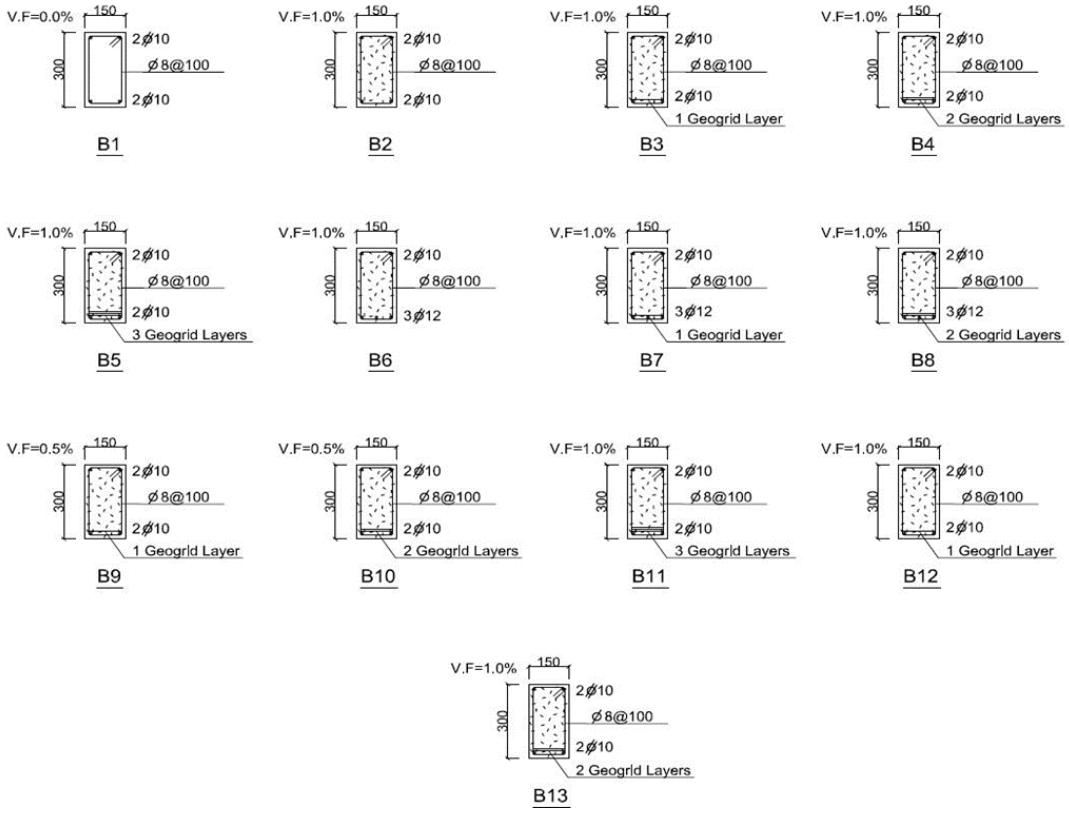


**Fig.4** Tested specimens geometry and details.

*3.2. Test setup*

The tested specimens were simply supported, 2100 mm long, with an effective span of 1900 mm. Test specimens were loaded at their middle with two-point loads 400 mm apart. The load was applied using a hydraulic jack monitored by a load cell of 500-ton capacity. Figure 5 shows the test set-up and instrumentation. Test specimens were tested to measure the ultimate loads, deflections, steel reinforcement strains, and geogrid strains. During testing, the deflections at the mid-span were measured with a linear variable displacement transducer "LVDT". The data was recorded by a computerized data logger.

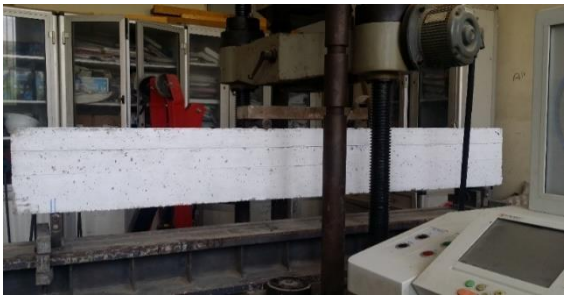

**Fig.5** Test set-up**.**

## 4. Experimental results and discussion

*4.1. Failure modes and crack patterns*

The specimens were experimentally tested for flexure by applying four-point loading tests. The failure type was recorded as a flexure failure for all beams. Generally, initial cracks for all tested beams appeared in the beam mid-span at the flexural region followed by consecutive cracks away from this region in the direction of supports with increasing loads. Increasing load values led to deeper and widened cracks with a major flexural crack in the maximum moment area at the failure load level. At failure, spalling of the concrete cover took place and the cover started to separate and pieces of concrete fell to the ground.

Using (1%) of steel fiber for the control specimen B2 delayed the appearance of the first cracking with reference to the non-fibrous specimen B1 by 39%.

Increasing the geogrid layers delayed the appearance of the first crack by 5% and 14% for beams B4 and B5 when compared to B3. Also, increasing the steel reinforcement ratios resulted in less spread cracks and less visual crack width.

Figure. 6 shows the failure modes of the tested beams.

**For group A:** For beams (B3), (B4), and (B5) reinforced with one, two, and three geogrid layers and a volume of steel fiber (1%); the initial crack appeared at the bottom surface at loads of 45, 47, and 51 kN. By increasing the load, cracks propagated up-to the specimen's top surface till the failure occurred at loads of 88, 95, and 101 kN. The failure type was recorded as a flexure failure for specimens B3, B4 and B5.

**For group B:** Beams (B6), (B7), and (B8) were reinforced with one, two, and three geogrid layers and a volume of steel fiber (1%) and reinforced with 3 Ø 12 as longitudinal steel reinforcement. The initial crack appeared at the bottom surface at loads of 65, 69, and 72 kN. As the load increased, cracks propagated until failure loads of 142, 146, and 153 kN. The failure type was recorded as a flexure failure for specimens B6 and B7. The failure type was recorded as a compression flexure failure for specimen B8.

**For group C:** Beams (B9), (B10), and (B11) were reinforced with one, two, and three geogrid layers and a volume of steel fiber (0.5%). The initial crack appeared at the bottom surface at loads of 35, 39, and 44 kN. As the load increased, cracks propagated until failure loads of 84, 89, and 94 kN. The failure type was recorded as a flexure failure for specimens B9, B10 and B11.

**For group D:** Beams (B12) and (B13) were reinforced with one and two geogrid layers (U-shaped) and a volume of steel fiber (1%). The initial crack appeared at the bottom surface at loads of 50 and 54 kN. As the load increased, cracks propagated until failure loads of 96 and 102 kN. The failure type was recorded as a flexure failure for specimens B12 and B13.


Specimen B1

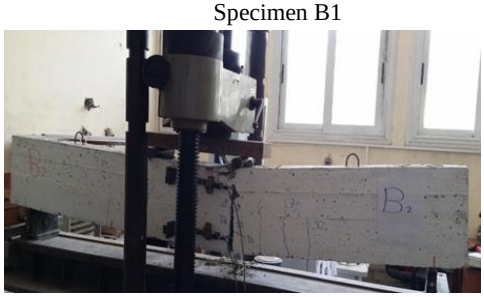


Specimen B2


Specimen B3


Specimen B4


Specimen B5

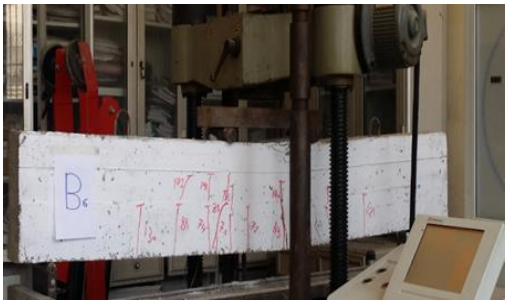


Specimen B6


Specimen B7


Specimen B8


Specimen B9

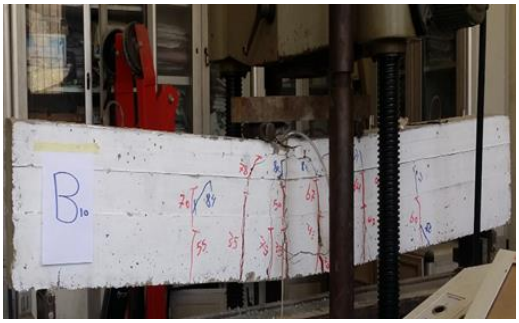


Specimen B10

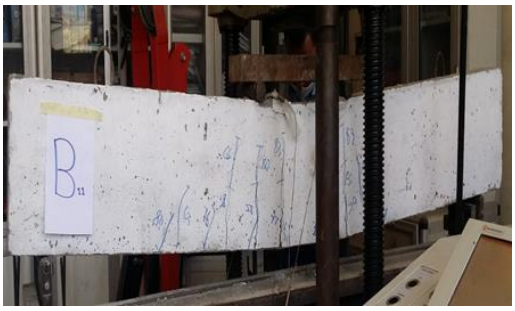


Specimen B11


Specimen B12


Specimen B13

**Fig.6** Crack pattern of the tested beams.

*4.2. Failure loads*

All specimens were tested up-to failure. The maximum load and the corresponding deflection at failure for the tested specimens were determined during the experimental program. Table 4 shows the experimental results for all the tested specimens.

4.2.1 Effect of the addition of geogrid layers on failure loads

The failure load of group (A) were increased by 7.3%, 15.9% and 23.2%, for beams B3, B4, and B5, respectively; compared to the control specimen B2. Group (C) were increased by 2.5%, 8.5% and 14.6%, for beams B9, B10, and B11 respectively; and for group (D) the increase was 17% and 24.4% for beams B12 and B13, respectively. Thus, the addition of geogrid layers had a significant effect on increasing the failure loads.

The failure load of group (B) (with 0.75% steel reinforcement) was increased by 73%, 78% and 86.6%, for beams B6, B7, and B8, respectively, compared to the control specimen B2.

4.2.2 Effect of increasing the number of geogrid layers on failure loads

Figure7. shows a comparison between the failure loads of B3 (reinforced with one layer of geogrid), B4 (reinforced with two layers of geogrid) and B5 (reinforced with three layers of geogrid). The failure load of B4 was increased by 7.9% compared to B3 while the failure load of B5 was increased by 14.8% compared to B3.

Figure7. shows a comparison between the failure loads of B9 (reinforced with one layer of geogrid and 0.5 % of steel fiber), B10 (reinforced

with two layers of geogrid and 0.5% of steel fiber) and B11 (reinforced with three layers of geogrid and 0.5% of steel fiber). The failure load of beams B10 and B11 were increased by 5.9% and 11.9% compared to B9.

Thus, increasing the number of geogrid layers has a considerable effect on increasing the failure loads.

4.2.3 Effect of the addition of steel fibers on the failure loads

Figure 7. shows a comparison between the failure load of the control specimen B1 (without steel fiber and without geogrid layers) and the failure load of the control specimen B2 (without geogrid layers but with 1% steel fiber). The failure load of specimen B2 was increased by 6.5% compared to the control specimen B1.

Increasing the fiber content, in the presence of geogrid layers, resulted in a slight increase of the failure loads for the specimens. Figure7. shows a comparison between group (A) and group (C). The failure load of B3 was increased by 4.7% compared to B9, the failure load of B4 was increased by 6.7% compared to B10 and the failure load of B5 was increased by 7% compared to B11.

Thus, the increase of fiber content from (0.5%) to (1%) have a slight effect on increasing the maximum carrying capacities of the beams.

4.2.4 Effect of the addition of U-shaped geogrid layers on the failure loads

Using (U)-shaped geogrid layers resulted in an increase of the failure loads for the specimens. Figure7. shows a comparison between group (A) and group (D). The failure load of B12 was increased by 9.1% compared to B3, and the failure load of B13 was increased by 7.4% compared to B4.

Thus, the addition of U-shaped geogrid layers has a considerable effect of increasing the failure load rather than the addition of geogrid layers in the tension zone only.

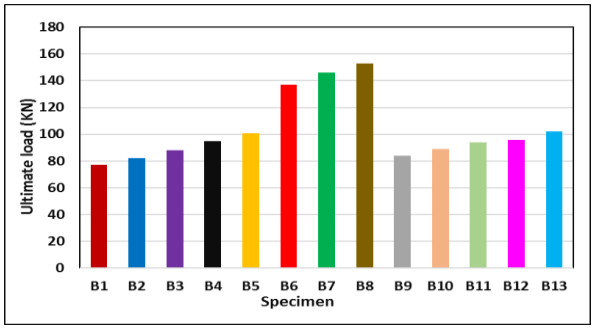


**Fig.7** Comparison of ultimate loads of specimens.

*4.3. Load-mid span deflection*

The comparison between each group of the specimens and the control specimens is plotted in Figure 8, 9, 10, and 11. These figures show the results of applied loads versus the mid-span deflection for the control beams with and without steel fiber and beams with and without layers of geogrid, respectively. Adding steel fiber in concrete results in a considerable decrease in deflection. The deflection at failure load for B2 equals was decreased by 9.7% compared to the control specimen B1.

**4.3.1** Effect of the addition of geogrid layers on deflection

Figure12. shows a comparison between the deflection of the control specimen B2 and the deflection of all specimens. The deflection of group (A) was decreased by 13.3%, 24% and 34.1%, for beams B3, B4, and B5, respectively, compared to the control specimen B2. The deflection of group (C) was decreased by 5.8%, 16.9% and 23.3%, for beams B9, B10, and B11, respectively, compared to the control specimen B2. The deflection of group (D) was decreased by 26% and 34.5%, for beams B12 and B13, respectively, compared to the control specimen B2.

Thus, the addition of geogrid layers had a significant effect on decreasing the deflections at failure loads.

The deflection of group (B) (with 0.75% main steel reinforcement) was decreased by 47.4%, 58.3% and 65.6%, for beams B6, B7, and B8, respectively, compared to the control specimen B2.

**4.3.2** Effect of increasing the number of geogrid layers on deflection

Figure12 shows a comparison between the deflection of B3, B4 and B5. The deflection of B4 was decreased by 12.3% compared to B3. The deflection of B5 was decreased by 23.9% compared to B3.

Figure12 shows a comparison between the deflection of B9, B10 and B11. The deflection of B10 was decreased by 11.8% compared to B9 while the deflection of B11 was decreased by 18.5% compared to B9.

Thus, using three layers of geogrid layers have a significant effect on decreasing the deflection.

**4.3.3** Effect of the addition of steel fibers on the deflection

Figure 12 shows a comparison between the deflection of the control specimen B1 and the deflection of the control specimen B2. The deflection of B2 is less than that of the control specimen B1 by 9.8%. Increasing the fiber content, in the presence of geogrid layers, resulted in a considerable decrease of deflection for the specimens. Figure 12 shows a comparison between group (A) and group (C). The deflection of B3 was decreased by 7.9% compared to B9. The deflection of B4 decreased by 8.5% compared to B10 while the deflection of B5 was decreased by 14% compared to B11.

Thus, the increase of fiber content from (0.5%) to (1%) have a considerable effect on decreasing the deflection.

**4.3.4** Effect of the addition of U-shaped geogrid layers on the deflection

Using U-shaped geogrid layers resulted in a decrease of deflection for the specimens. Fig.12 shows a comparison between group (A) and group (D). The deflection of B12 was decreased by 14.6% compared to B3 and the deflection of B13 was decreased by 13.8% compared to B4.

Thus, the addition of U-shaped geogrid layers have a considerable effect on decreasing the deflection rather than the addition of geogrid layers in the tension zone only.

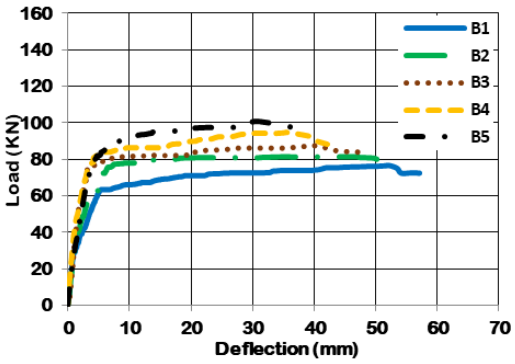


**Fig.8** Load-deflection curve of a group (A)

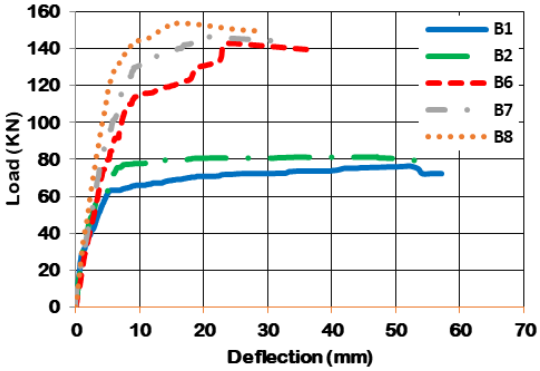


**Fig.9** Load-deflection curve of a group (B).

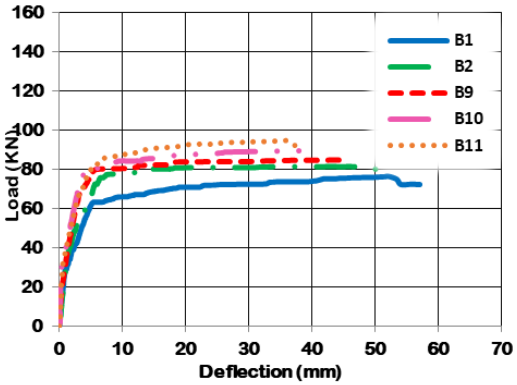


**Fig.10** Load-deflection curve of a group (C)

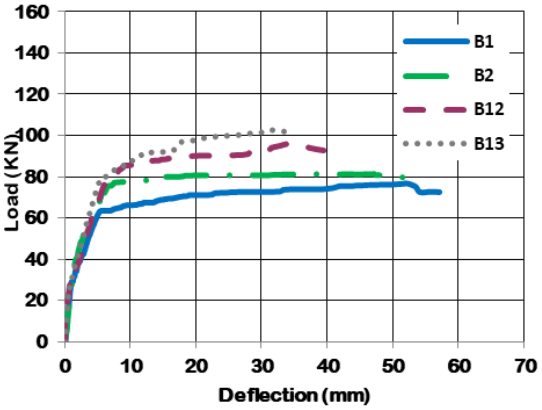


**Fig.11** Load-deflection curve of a group (D).

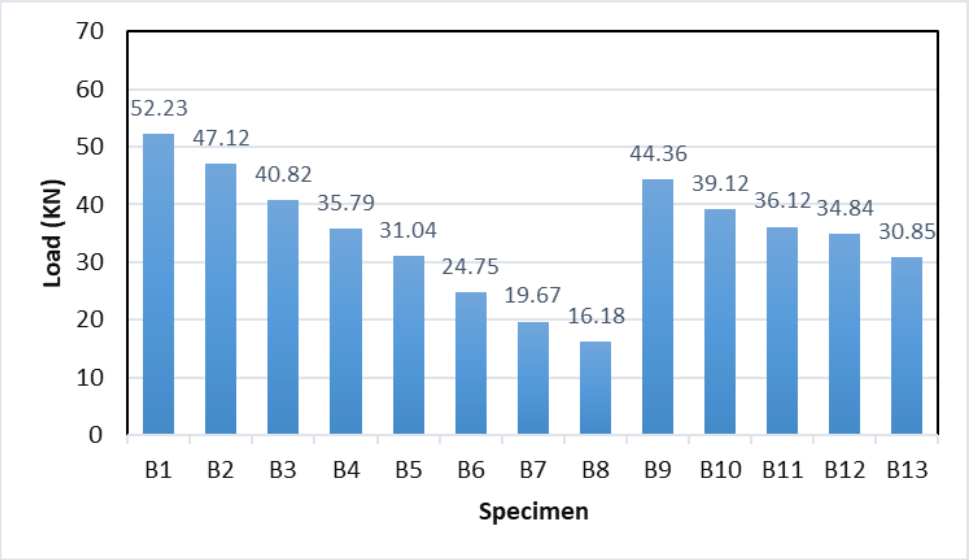


**Fig.12** Comparison of ultimate deflections of specimens.

**Table 4.** Test results.

| Group | Specimen | First Crack Load (kN) | Failure Load (kN) | Load Enhancement Ratio Compared to B2 | Ultimate Deflection (mm) | Deflection Decreases Ratio Compared to B2 | Ductility Ratio | Energy Absorption (kN.mm) |
|---|---|---|---|---|---|---|---|---|
| **Control** | B1 | 30 | 77 | --- | 52.23 | --- | 9.65 | 3758.8 |
| **Control** | B2 | 42 | 82 | --- | 47.12 | --- | 7.83 | 3513.8 |
| **A** | B3 | 45 | 88 | 7.3 | 40.82 | 13.3 | 6.99 | 3306.2 |
| | B4 | 47 | 95 | 15.9 | 35.79 | 24 | 5.42 | 3119.5 |
| | B5 | 51 | 101 | 23.2 | 31.04 | 34.12 | 3.44 | 2750.9 |
| **B** | B6 | 65 | 142 | 73 | 24.75 | 47.4 | 2.80 | 2539.2 |
| | B7 | 69 | 146 | 78 | 19.67 | 58 | 2.18 | 2033.1 |
| | B8 | 72 | 153 | 86.6 | 16.18 | 65.6 | 1.90 | 1659 |
| **C** | B9 | 35 | 84 | 2.5 | 44.36 | 5.8 | 7.27 | 3496.6 |
| | B10 | 39 | 89 | 8.5 | 39.12 | 16.9 | 5.82 | 3315.2 |
| | B11 | 44 | 94 | 14.6 | 36.13 | 23.3 | 3.46 | 3089.5 |
| **D** | B12 | 50 | 96 | 17 | 34.84 | 26 | 3.01 | 3252.9 |
| | B13 | 54 | 102 | 24.4 | 30.85 | 34.5 | 1.78 | 2824.9 |

*4.4. Energy Absorption (Toughness)*

Toughness is the area under curve up to fracture, as shown in Fig.13. The presence of geogrids and steel fiber in the beams results in a significant decrease in its toughness. The toughness of the control beam (B1) was decreased by 6.5% compared to the control beam B2. The toughness for group A (beams B3, B4, and B5) was smaller than that of B2, respectively, by 5.9 %, 11.2%, and 21.7%.

For group (B), the toughness for B6, B7, and B8 was smaller than B2, respectively, by 27 %, 42.2 %, and 52.8 %. For group (C), the toughness for B9, B10, and B11 was smaller than B2, respectively, by 3 %, 5.6 %, and 12%. For group (D), the toughness for B11 and B12 was smaller than B2, respectively by 7.4% and 19.5%.

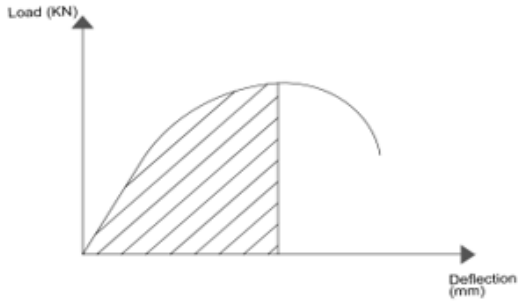


**Fig.13** Toughness

*4.5. Ductility*

Ductility is the ability of a material to sustain plastic deformation before failure. Ductility is a special form of deformability. Ductility has many definitions, among standard inductors of ductility is the ratio between deflection at failure and deflection at yield load. This inductor is shown in Table 5.

Ductility=Δ_ultimate/Δ_yield

**Table 5**. Comparison of ductility ratio of specimen's test results.

| Test beam | $\Delta_{yield}$ (mm) | $\Delta_{ultimate}$ (mm) | Ductility ratio | |
|---|---|---|---|---|
| | | | Absolute | Relative to B1 |
| B1 | 5.40 | 52.23 | 9.65 | 1 |
| B2 | 6.01 | 47.12 | 7.83 | 0.81 |
| B3 | 5.83 | 40.82 | 6.99 | 0.72 |
| B4 | 6.60 | 35.79 | 5.42 | 0.56 |
| B5 | 8.99 | 31.04 | 3.44 | 0.36 |
| B6 | 8.82 | 24.75 | 2.80 | 0.3 |
| B7 | 8.99 | 19.67 | 2.18 | 0.23 |
| B8 | 8.48 | 16.18 | 1.90 | 0.2 |
| B9 | 6.10 | 44.36 | 7.27 | 0.76 |
| B10 | 6.71 | 39.12 | 5.82 | 0.61 |
| B11 | 10.43 | 36.13 | 3.46 | 0.36 |
| B12 | 11.54 | 34.84 | 3.01 | 0.31 |
| B13 | 17.25 | 30.85 | 1.78 | 0.18 |

*4.6. Nominal moment*

The experimental moment capacity ($M_{exp.}$) for all the beams was estimated using the equation (P/2*0.75=0.375 P kN.m) [31], where P is the failure load and the shear span equals 0.75 m. the experimental results were compared with that calculated ACI design code equations [32]. ACI-code 318–19 [32] presented an equation to calculate the nominal moment ($M_n$) of an R.C rectangular beam of a cross-section (b*t). The assumptions to predict the nominal flexural strength were considered. The equilibrium equation can be calculated as follows:

$$C_c=T_s+T_f+T_g \quad (1)$$

The compression force of concrete ($C_c$) can be calculated depending on the rectangular cross section which is estimated as:

$$C_c=\sigma_{ec}*A_c \quad (2)$$

The compressive strength of concrete ($\sigma_{ec}$) can be defined as:

$$\sigma_{ec}=\alpha*f_{cu} \quad (3)$$

According to ACI-code 318–19 [32], the coefficient (α) is assumed to be 0.85. Also, the area of compression zone ($A_c$) was calculated as:

$$A_c=b*a \quad (4)$$

The depth of the rectangular cross section (a) was calculated as:

$$a=\beta*C \quad (5)$$

Factor (b) should not be more than 0.85 and should not be less than 0.65 [32]. It was calculated as:

$$\beta=0.85-0.05[(f_{cu}-28)/7] \quad (6)$$

$C_c$ can be defined as:

$$C_c=0{:}85*f_{cu}*b*a \quad (7)$$

$$T_s=A_s*f_y \quad (8)$$

$$T_f=1.64V_f*(L_f/\Phi)b(t-c) \quad (9)$$

$$T_g=A_g*f_g \quad (10)$$

According to ACI Committee 544 [33]. $\sigma_t$ can be estimated as:

$$\sigma_t=0.00772*L/d_f*p_f*f_{be} \quad (11)$$

The bond efficiency of the fiber ($f_{be}$) varies from 1.0 to 1.2 depending upon fiber characteristics [34].

The nominal moment ($M_n$) can be estimated as:

$M_n=[(A_s*f_y+A_g*f_g)][d-a/2]+\sigma_t*b(t-e)*[t/2+e/2+a/2]$[31] (12)

The analysis procedure for calculating Mn. can be easily implemented by hand calculations or a spreadsheet. Mn. was calculated for all beam specimens using Eq. (12).

Table 6 shows the comparison of the experimental and the nominal flexural strength.

The conclusions found that good agreement between the nominal and the experimental flexural strength. The average ratio of [Mu, exp./Mn.] for the tested

beams are 1.045 with 0.282 standard deviation.

## 5. Conclusions

For the range of the studied parameters, the major conclusions derived from this research can be summarized as follows:

1. Addition of uniaxial geogrids as a reinforcing technique proved to be an effective tool to improve the beams' flexural behavior and improve the cracking patterns.
2. Addition of geogrid layers has a significant effect of increasing the failure loads. The failure load increased by 7.3%, 15.9% and 23.2% by adding one, two and three geogrid layers respectively, compared to the control specimen without any geogrid layers.
3. Using geogrid layers has a significant effect on decreasing the deflection. The deflection of group (A) was decreased by 13.3%, 24% and 34.1%, by adding one, two and three geogrid layers respectively, compared to the control specimen without any geogrid layers.
4. Addition of geogrid layers as U-shaped has a considerable effect on increasing the failure load compared to the addition of geogrid layers in the tension zone only. By using U-shaped geogrid layers, the failure load increased by 17% and 24.4% by adding one and two U-shaped geogrid layers respectively, compared to the control specimen without any geogrid layers.
5. Addition of geogrid layers as U-shaped has a considerable effect on decreasing the deflection compared to the addition of geogrid layers in the tension zone only. By using U-shaped geogrid layers, the deflection decreased by 26% and 34.5% by adding one and two U-shaped geogrid layers respectively, compared to the control specimen without any geogrid layers.
6. Addition of steel fiber in R.C beams increases the cracking loads, failure loads and reduces the deflection of beams at failure loads.
7. Increasing the fiber content from (0.5%) to (1%) increases the failure load of the beams slightly in the presence of geogrid layers. Increasing the fiber content increases the failure load by 5%, 7 % and 8% when one, two and three layers were used respectively.
8. Increasing the fiber content from (0.5%) to (1%) had a considerable effect of decreasing the maximum deflection of the beams. Increasing the fiber content decreased the maximum deflection by 8%, 8.5 % and 14 % when one, two and three layers were used respectively.

**Nomenclature**

| | |
|---|---|
| $A_c$ | The area at compression zone. |
| $A_s$ | The area of steel reinforcement bars in tension-zone. |
| $A_g$ | The area of uniaxial geogrid. |
| a | The depth of the rectangular cross section. |
| b | Width of the cross-section. |
| C | Depth of the compression zone in concrete. |
| $C_c$ | The compression force at concrete. |
| d | Depth of the beam. |
| $d_f$ | Fiber diameter. |
| e | Depth of the concrete at tension zone. |
| $F_{be}$ | The steel fiber bond efficiency. |
| $f_u$ | The ultimate strength of the reinforcing bars. |
| $f_y$ | The yield strength of the reinforcing bars. |
| $f_g$ | The tensile strength of the uniaxial geogrid. |
| $I$ | Energy absorption. |
| $L$ | Length of the beam. |
| $l_f$ | Length of steel fibers. |
| $M_{exp.}$ | Experimental moment strength. |
| $M_n$ | Nominal flexural strength. |
| $T_s$ | Steel reinforcing bars' tension force. |
| $T_f$ | Steel fibers' tension force. |
| $T_g$ | Tension force of the used geogrid. |
| $t$ | The depth of the cross section. |
| $V_f$ | Volume of fibers. |
| $X$ | Flexural shear span. |
| $\alpha$ | Coefficient defined by the design code. |
| $\beta$ | Equivalent rectangular factor relating depth. |
| $\sigma_t$ | The tensile stress of fibrous concrete. |

**Table.6** Nominal and Experimental Flexural Strength.

| Beam | Fcu MPa | Geometrical Parameters | | | | | Bottom RFT | | | | | | Mexp. kN.m | Mn kN.m) | Mexp. /Mn |
|---|---|---|---|---|---|---|---|---|---|---|---|---|---|---|---|
| | | b (mm) | d (mm) | L (mm) | x (mm) | As HTS | Fy MPa | Vf % | l/d | Ag ($mm^2$) | Fg MPa | | | | |
| B1 | 40 | 150 | 275 | 2100 | 750 | 2Ø10 | 360 | 0 | --- | --- | --- | | 25 | 16 | 1.5 |
| B2 | 40 | 150 | 275 | 2100 | 750 | 2Ø10 | 360 | 1 | 50 | --- | --- | | 26.6 | 17.8 | 1.4 |
| B3 | 40 | 150 | 275 | 2100 | 750 | 2Ø10 | 360 | 1 | 50 | 144 | 160 | | 28.6 | 24.1 | 1.2 |
| B4 | 40 | 150 | 275 | 2100 | 750 | 2Ø10 | 360 | 1 | 50 | 288 | 160 | | 30.9 | 30.2 | 1.02 |
| B5 | 40 | 150 | 275 | 2100 | 750 | 2Ø10 | 360 | 1 | 50 | 432 | 160 | | 32.8 | 36.5 | 0.8 |
| B6 | 40 | 150 | 275 | 2100 | 750 | 3Ø12 | 360 | 1 | 50 | --- | --- | | 46.2 | 35.6 | 1.3 |
| B7 | 40 | 150 | 275 | 2100 | 750 | 3Ø12 | 360 | 1 | 50 | 144 | 160 | | 47.5 | 41.8 | 1.1 |
| B8 | 40 | 150 | 275 | 2100 | 750 | 3Ø12 | 360 | 1 | 50 | 288 | 160 | | 49.7 | 47.9 | 1 |
| B9 | 40 | 150 | 275 | 2100 | 750 | 2Ø10 | 360 | 0.5 | 50 | 144 | 160 | | 27.3 | 22.7 | 1.2 |
| B10 | 40 | 150 | 275 | 2100 | 750 | 2Ø10 | 360 | 0.5 | 50 | 288 | 160 | | 28.9 | 28.8 | 1 |
| B11 | 40 | 150 | 275 | 2100 | 750 | 2Ø10 | 360 | 0.5 | 50 | 432 | 160 | | 30.5 | 35 | 0.87 |
| B12 | 40 | 150 | 275 | 2100 | 750 | 2Ø10 | 360 | 1 | 50 | 624 | 160 | | 31.2 | 44.8 | 0.7 |
| B13 | 40 | 150 | 275 | 2100 | 750 | 2Ø10 | 360 | 1 | 50 | 1248 | 160 | | 33.15 | 68 | 0.5 |
| | | | | | | | | | | | | Average | | | 1.045 |
| | | | | | | | | | | | | Standard deviation | | | 0.282 |

## 6. References


[1] Tang, X., Chehab, G.R.and Palomino, A.,"Evaluation of Geogrids for Stabilising Weak Pavement Subgrade," International Journal of Pavement Engineering. 2008, Vol. 9, no. 6, pp 413–429.

[2] Abu-Farsakh, M.Y., Akond, I. and Chen, Q.," Evaluating the Performance of Geosynthetic-Reinforced Unpaved Roads Using Plate Load Tests," International Jornal of Pavement EngIneering, 2016, Vol. 17, no. 10, pp 901–912.

[3] Reddy, P.M.and Kumar, J.R.," Study of Geogrid Confined Reinforced Concrete Beams," International Journal. Science Engineering Technology. Research. (IJSETR) 2018, Vol. 7, no. 4, pp 278–286.

[4] El Meski, F., Chehab, G.," Flexural Behavior of Concrete Beams Reinforced with Different Types of Geogrids", Journal of Materials in Civil Engineering. 2014, Vol. 26, no. 8, 04014038.

[5] Arulrajah, A, Rahman, M.A.Piratheepan, J.,Bo, M. and Imteaz, M. "Evaluation of Interface Shear Strength Properties of Geogrid-

Reinforced Construction and Demolition Materials Using a Modified Large-Scale Direct Shear Testing Apparatus" Journal of Materials in Civil Engineering. 2014, Vol. 26, no. 5, 974–982.

[6] Abdesssemed, M., Kenai, S. and Bali, A.," Experimental and Numerical Analysis of the Behavior of an Airport Pavement Reinforced by Geogrids," Constrtruction. and Building Materials. 2015, Vol. 94, no. 5, pp 547–554.

[7] Chidambaram, R.S. and Agarwal, P.,"The Confining Effect of Geogrid on the Mechanical Properties of Concrete Specimens with Steel Fiber under Compression and Flexure,"Construction Building Materials, 2014,Vol. 71, pp 628–637.

[8] Chidambaram, R.S. and Agarwal, P.,"Flexural and Shear Behavior of Geogrid Confined RC Beams with Steel Fiber Reinforced Concrete,"Construction Building Materials, 2015, Vol. 78, pp 271–280.

[9] Siva Chidambaram, R. and Agarwal, P.,"Inelastic Behaviour of RC Beams with Steel Fiber and Polymer Grid Confinement," Indian Concrete Journal, 2015, Vol. 89, no. 4, pp83–90.

[10] Wang, W., Sheikh, M.N.; and Hadi, M.N.,"Axial Compressive Behaviour of Concrete Confined with Polymer Grid," Materials and Structures, 2016, Vol.49, no. 9, pp 3893–3908.

[11] Tang, X., Higgins, I. and N Jlilati, M.,"Behavior of Geogrid Reinforced Portland Cement Concrete under Static Flexural Loading," Infrastructures, 2018, Vol. 3, no. 4, pp 41.

[12] Chalioris, C.E., Zapris, A.G. and Karayannis, C.G.,"U-Jacketing Applications of Fiber Reinforced Polymers in Reinforced Concrete T-Beams against Shear Tests and Design," Fibers, 2020, Vol. 8, no. 2, pp 13.

[13] Abdulhameed, A.A. and Said,A.I.,"CFRP Laminates Reinforcing Performance of Short-Span Wedge-Blocks Segmental Beams," Fibers, 2020, Vol. 8, no. 1, pp 6.

[14] Jaafer, A.A., AL-Shadidi, R. and Kareem, S.L.,"Enhancing the Punching Load Capacity of Reinforced Concrete Slabs Using an External Epoxy-Steel Wire Mesh Composite,"Fibers, 2019, Vol. 7, no. 8, pp 68.

[15] Chalioris, C.E., Kosmidou, P.-M.K. and Papadopoulos, N.A.," Investigation of a New Strengthening Technique for RC Deep Beams Using Carbon FRP Ropes as Transverse Reinforcements,"Fibers, 2018, Vol. 6, no. 3, pp 52

[16] Itani, H., Saad, G. and Chehab, G.," The Use of Geogrid Reinforcement for Enhancing the Performance of Concrete Overlays," Construction and Building Materials, 2016, Vol. 124, PP 826–837.

[17] Maxwell, S., Kim,W., Edil, T. B., and Benson, C. H. "Effectiveness of Geosynthetics in Stabilizing Soft Subgrades," Final Rep. No. 0092- 45-15, Dept. of Civil and Environmental Engineering, Univercity. of Wisconsin-Madison, 2005.

[18] Cancelli, A., Montanelli, F., Rimoldi, P., and Zhao, A. "Full Scale Laboratory Testing on Geosynthetics Reinforced Paved Roads," Proceedings of the International Symposium on Earth Reinforcement, Fukuoka, Kyushu, Japan, 1996, pp. 573-578.

[19] Santoni, R., L., Smith, C., J., Tingle, J.S., and Webster, S.L. "Expedient Road Construction Over Soft Soils" Technical Report TR-01-7, U.S. Army Engineer Research and Development Center, Waterways Experiment Station, Vicksburg, MS, 2001.

[20] Al-Hedad, A.S., Bambridge, E. and Hadi, M.N.," Influence of Geogrid on the Drying Shrinkage Performance of Concrete Pavements," Construction and Building Materials, 2017, Vol. 146, pp 165–174.

[21] Chidambaram, R.S. and Agarwal, P.," The Confining Effect of Geogrid on the Mechanical Properties of Concrete Specimens with Steel Fiber under Compression and Flexure," Construction and Building Materials, 2014, Vol.71, pp 628–637.

[22] Kim, S., Tang, X. and Chehab, G.R.,"Laboratory Study of Geogrid Reinforcement in Portland Cement Concrete" In Pavement Cracking: Mechanisms, Modeling, Detection, Testing and Case Histories; CRC Press: Boca Raton, FL, USA, 2008; pp. 769–778.

[23] Chand Beebi, D. and VisweswaraRao, V.K.., "Flexural Behavior of Geo-Grid Reinforced Concrete", International Journal for Research in Applied Science and Engineering Technology (IJRASET), Vol. 5, Issue X, October 2017, pp 7-15.

[24] Santosh Chaudhari, D Rajitha, and K Chandra Mouli., " Flexural Behavior of Geopolymer Concrete Beams Using Geogrid", International Journal of Civil Engineering and Technology (IJCIET), Vol. 8, Issue 12, December 2017, pp 224–232.

[25] Shobana S. and Yalamesh G., "Experimental Study of Concrete Beams Reinforced with Uniaxial and Biaxial Geogrids", International Journal of Chem-Tech Research , Vol. 8, no. 3, 2015, pp 1290-1295.

[26] Rakendu K. and Anagha Manoharan, "Flexural Behavior of Concrete Beams Reinforced with Biaxial Geogrid", International Journal of Engineering Research and General Science, Vol. 5, no. 4, July-August, 2017, pp 72-83.

[27] Sujesh G., Aniket M., Durvesh D. , Jatin S. , and Mohd. F., "Comparative Study and Analysis of PCC Beam and Reinforced Concrete Beam using Geogrid", International Journal of Science Technology and Engineering (IJSTE), Vol. 3, no. 11, May 2017, pp 247-253.

[28] Ahmed Shaban Abdel-Hay Gabr, "Strengthening of Reinforced of Concrete Slabs Using Different Types of Geo-grids", International Journal of Civil Engineering and Technology (IJCIET), 2019, Vol. 10, no. 1, pp. 1851-1861.

[29] Abeer M. Erfan, Tamer H. K. Elafandy, Mahmoud M. Mahran and Mohamed Said., "Behavior of Self Compacted Concrete Ferrocement Beams", Journal of Engineering Research and Reports, JERR., 2021, pp 1-14.

[30] Egyptian Code of Practice: Design and construction of reinforced concrete structures, (ECCP 203-2020).

[31] Ali S. S., Mohamed S., Alaa I., A., and Amira M., "Flexural performance of concrete beams containing engineered cementitious composites", Construction and Building Materials, 2018, Vol. 180, pp 23-34.

[32] ACI Committee 318-19, Building Code Required for Structural Concrete, (ACI 318-19) and Commentary (ACI 318R-19), American Concrete Institute, Farmington Hills, Michigan, 2019.

[33] ACI Committee 544, Design considerations for steel fiber reinforced concrete;(ACI 544.4R-88). Farmington Hills (Michigan, MI): American Concrete Institute; 1988. Re-approved 1999, 1999.

[34] Mohamed S., Tarek S., M., Ali S. S., and Mostafa M. K., "Experimental and analytical investigation of high performance concrete beams reinforced with hybrid bars and polyvinyl alcohol fibers", Construction and Building Materials, Vol. 259, 2020.